Structural and Functional Characterization of Enzyme-Quantum Dot Conjugates: Covalent Attachment of CdS Nanocrystal to α-Chymotrypsin

S. Shankara Narayanan, Rupa Sarkar, and Samir Kumar Pal*

Unit for Nano Science & Technology, Department of Chemical, Biological & Macromolecular Sciences, S. N. Bose National Centre for Basic Sciences, Block JD, Sector III, Salt Lake, Kolkata 700 098, India

Received: April 4, 2007; In Final Form: May 18, 2007

In this contribution, we report the synthesis of CdS nanoparticles directly conjugated to an enzyme, α-chymotrypsin (CHT) by chemical reduction in aqueous solution. Matrix-assisted laser desorption ionization (MALDI) mass spectrometry confirms the strong conjugation of CdS nanoparticles to CHT through covalent bonding in the CdS−CHT conjugates. High-resolution transmission electron microscopy (HRTEM) reveals that the CdS nanoparticles are well dispersed with an average diameter of 3 nm, and energy dispersive X-ray elemental analysis (EDAX) verifies the composition of the CdS−protein conjugates. The structural integrity of CHT before and after the conjugation of CdS nanoparticles is confirmed through circular dichroism (CD) studies. The functional integrity of CHT conjugated to CdS nanoparticles is investigated by monitoring the enzymatic activities of CHT and CHT-conjugated CdS nanoparticles by using absorption spectroscopy. The attachment of CdS nanoparticles to an enzyme with its structural and functional integrity may have impact in the future research on nanobio interface.

Introduction

Over the past decades, semiconductor nanoparticles (NPs) have been studied in detail owing to their unique size-dependent optical and electrical properties.[1,2] Their synthesis and characterization have attracted much attention due to the broad applicability of these unique materials in a myriad of areas such as optics and opto-electronics,[3−5] photocatalysis,[6] biological labeling,[7,8] and molecular biology.[9−13] As NPs are being explored for various novel applications, considerable efforts for devising more efficient protocols for the synthesis of uniform size NPs have followed.[14−19] Many of these approaches utilize organic capping ligands such as tri-n-octylphosphine[15,16] and restricted nanoenvironments like reverse micelles[17,18] and phospholipid vesicles.[19]

Bioconjugate synthesis of inorganic NPs using biomolecules such as proteins and DNA[20,21] has recently aroused great interest due to the broad range of applications of such hybrid materials from life sciences to materials and nanosciences. The motivation is based on the unique properties of the inorganic nanoparticles possessing strongly size-dependent optical, electrical, magnetic, and electrochemical properties combined with the perfect binding and biochemical functionality of biomacromolecules. Particularly, proteins have been extensively employed to extend the binding capabilities of inorganic nanoparticles.[7,8,22,23] Protein-assisted synthesis of nanoparticles is a potent method for the creation of uniform particle size.[14] There have been various reports employing different proteins to prepare NPs.[24−29] Particularly, semiconductor nanoparticles with uniform particle size have been widely reported. For instance, the cage-shaped protein, apoferritin has been employed as a size-restraining chemical reaction chamber for the synthesis of uniform size nickel and cadmium,[30] CdS[25] and CdSe[26] nanoparticles. In another study, CdS nanocrystals with small-disperse size have been synthesized in pepsin solution by designing a slow chemical reaction system of Cd^{+2} and S^{-2}.[27] However, in the recent literature, much less attention has been paid on the structural and functional aspects of the proteins after the attachment of the nanoparticles.[31−35]

In the present study, we have synthesized water-soluble CdS nanoparticle of 3 nm average diameter directly conjugated to an enzyme bovine pancreatic α-chymotrypsin (CHT). We obtain a well-dispersed, protein-conjugated CdS nanoparticle that remained stable indefinitely in solution. The structural and size characterization of CHT-conjugated CdS nanoparticles was done by using steady state absorption/photoluminescence (PL) spectroscopy, MALDI mass spectrometry, and high-resolution transmission electron microscopy (HRTEM). Studies are carried out in which the functionality of CHT and CdS nanoparticles conjugated to CHT is compared by monitoring their enzymatic activities on a substrate.

Materials and Methods

Anhydrous $Na_2S{\cdot}9H_2O$, $Cd(NO_3)_2$ $4H_2O$, bovine pancreatic α-chymotrypsin (CHT), tris(2-carboxyethyl)phosphine hydrochloride (TCEP), Ala−Ala-Phe 7-amido-4-methyl coumarin (AAF-AMC) were obtained from Sigma Aldrich. The chemicals and the proteins are of highest commercially available purity and were used as received. All aqueous solutions were prepared using double distilled water from a Millipore system. The synthesis of CHT-conjugated CdS NPs was carried out by chemical reduction in aqueous solution using TCEP as a reducing agent at ambient conditions. All aqueous solutions were deoxygenated by argon gas, and the reactions were carried out under an inert atmosphere to prevent oxidation of thiols back to disulfides.[36] The typical procedure for the synthesis of conjugated CdS NPs is as follows: 4 mL of 100 μM CHT aqueous solution was prepared and dialyzed exhaustively against water (pH = 4.5) at 4 °C. This was carefully degassed with argon gas for 45 min. The reducing agent TCEP[36−38] (80 μL of

* Corresponding author. E-mail: skpal@bose.res.in. Fax: 91 33 2335 3477.

10.1021/jp072636j CCC: $37.00 © 2007 American Chemical Society
Published on Web 07/10/2007

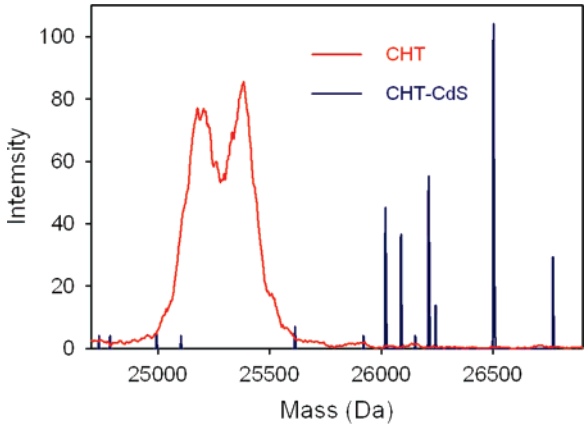

Figure 1. MALDI-mass spectra of CHT and CHT−CdS conjugates.

150 mM) was then added to the above protein solution and stirred continuously for 15 min under an argon blanket. It is well-known that the reduction of solvent exposed disulfides by TCEP proceeds readily at low pH.[37] The pH of CHT solution was maintained at 4.5 since TCEP reduces disulfides rapidly and cleanly in water at pH = 4.5 at room temperature.[37] At these values of pH, thiolate-disulfide interchange is effectively prevented because only low levels of thiolate are present. It is therefore possible to generate thiol from disulfide with kinetic selectivity under conditions in which thiolate-disulfide interchange does not occur.[37] At the TCEP concentration we have used (3 mM), the reduction of disulfides is complete within 5 min. A degassed aqueous Cd^{+2} solution (150 mM) was then added to the above solution (containing CHT and TCEP) and vigorously stirred for 30 min. This was followed by dropwise addition of aqueous S^{-2} solution (150 mM) with vigorous stirring. The final concentration of Cd^{+2} and S^{-2} in the aqueous solution was maintained to be 20 and 10 mM respectively. The reaction was allowed to proceed for 3 h, and the final solution was centrifuged. The resultant supernatant was filtered and then dialyzed against water of pH = 4.5 at 4 °C to remove any excess of salts and TCEP left in the solution. The final dialyzed solution was collected and stored at 4 °C prior to analysis. The molar ratio of CdS:CHT was found to be approximately 1:1 from the absorption spectrum of CdS−CHT conjugate.

UV−vis absorption spectroscopy and steady-state photoluminescence (PL) were done using Shimadzu model UV-2450 spectrophotometer and Jobin Yvon model Fluoromax-3 fluorimeter respectively. A JEOL JEM-2100 high-resolution transmission electron microscopy (HRTEM) equipped with an energy dispersive X-ray (EDAX) spectrometer was used to characterize the internal structures of samples and to analyze their elemental composition. Matrix-assisted laser desorption ionization (MALDI) mass spectra were obtained using an Applied Biosystem Voyager-DE PRO mass spectrometer. The circular dichroism study was done using Jasco 815 spectropolarimeter using a quartz cell of path-length 10 mm. All of the photoluminescence transients were taken using the picosecond-resolved time-correlated single photon counting (TCSPC) technique. We used a commercially available picosecond diode laser-pumped (LifeSpec-ps) time-resolved fluorescence spectrophotometer from Edinburgh Instruments, U.K. The picosecond excitation pulse from the picoquant diode laser was used at 375 nm with instrument response function (IRF) of 80 ps. A microchannel-plate-photomultiplier tube (MCP−PMT, Hammamatsu) was used to detect the photoluminescence from the sample after dispersion through a monochromator. For all transients, the polarizer on the emission side was adjusted to be at 55° (Magic

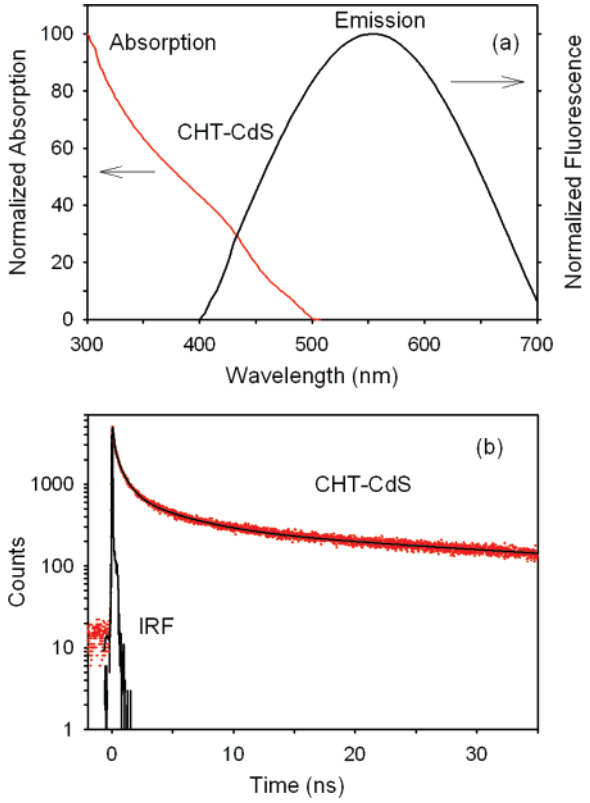

Figure 2. (a) UV−vis absorption and steady-state photoluminescence (PL) spectra of CdS−CHT conjugates. (b) Picosecond-resolved transient of CdS−CHT conjugates.

angle) with respect to the polarization axis of the excitation beam. The observed fluorescence transients were fitted by using a nonlinear least-square fitting procedure to a function ($X(t) = \int_0^t E(t')\, R(t - t')\, dt'$) comprising of convolution of the IRF (E(t)) with a sum of exponentials ($R(t) = A + \sum_{i=1}^{N} B_i e^{-t/\tau_i}$) with preexponential factors (B_i), characteristic lifetimes (τ_i) and a background (A). Relative concentration in a multiexponential decay is finally expressed as, $c_n = B_n/(\sum_{i=1}^{N} B_i) \times 100$.

Catalytic measurements in our experiment were made using the substrate AAF-AMC. The extinction coefficient used for determining the concentration of AAF-AMC in buffer (10 mM, pH = 7.0) is 16 mM^{-1} cm^{-1} at 325 nm.[39] For the enzymatic kinetics experiment, the concentration of CHT and CHT−CdS was maintained at 20 μM, whereas that of substrate was maintained at 200 μM. The rate of formation of product was monitored by observing the change in the absorbance at 370 nm of the product with time.

Results and Discussion

The covalent binding of CdS to CHT was confirmed by MALDI-mass spectra analysis (Figure 1). An average peak at 25288 Da corresponds to the molecular mass of CHT, which shifts to a major peak at 26502 Da for the CdS-conjugated CHT. The increase of the mass of CdS−CHT conjugates by 1214 Da as compared to pure CHT corresponds to approximately 9 CdS (formula weight of CdS is 144) molecule or equivalently 18 atoms in the CdS nanocrystal. The effective diameter, d, of the nanocrystals is calculated assuming that the particles are spherical in shape using the formula[40]

$$d = \left[\frac{3N_{at}a^2c}{2\pi}\right]^{1/3}$$

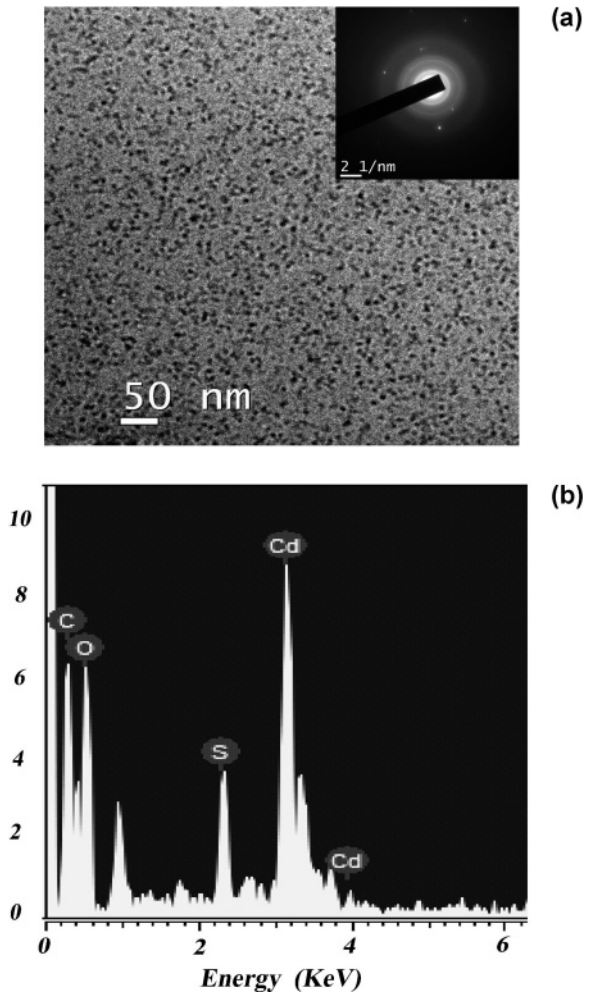

Figure 3. (a) High-resolution transmission electron micrograph (HRTEM) of CdS−CHT conjugates. Inset shows selected area electron diffraction (SAED) pattern of CdS−CHT conjugates. (b) Energy dispersive X-ray (EDAX) spectra of CdS−CHT conjugates.

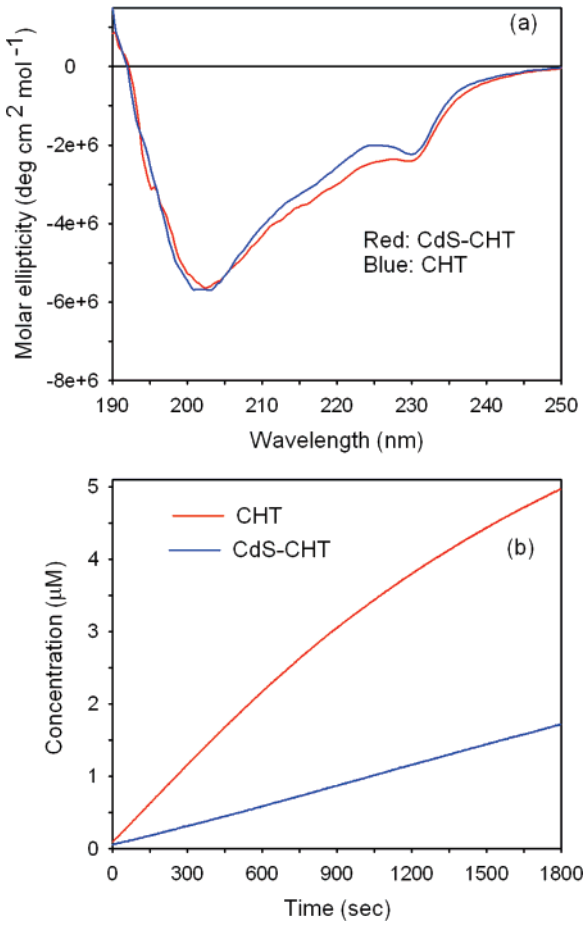

Figure 4. (a) Circular dichroism (CD) spectra of CHT and CdS−CHT conjugates. (b) Enzymatic activities of CHT and CdS−CHT on the substrate, AAF-AMC.

where $a = 4.12$ Å and $c = 6.65$ Å are the bulk lattice parameters and N_{at} is the number of atoms in the nanocrystal. The estimation of the diameter of the CdS nanocrystals with $N_{at} = 18$ atoms using the above formula reveals an average value of 1.0 nm on considering the crystal structure to be Wurzite (see below). Figure 2a shows the UV−vis absorption and photoluminescence (PL) spectra of the conjugated CdS nanoparticles. The absorption spectrum reveals a band centered at 400 nm, which indicates a relatively narrow size distribution. The absorption edge (472 nm) is clearly blue-shifted with respect to the bulk CdS (~515 nm), due to the quantum size effect of nanocrystals.[41,42] The particle size estimated using the Henglein's empirical formula[1,43] is 4 nm and the estimated band gap using effective mass model[44] is 2.64 eV. The PL spectrum of CHT−CdS (Figure 2a) reveals an emission band centered at 550 nm, which is attributed to the recombination of charge carriers within surface states. To examine the effect of excitation wavelengths on the observed photoluminescence from the nanoparticles, we used excitation from 350 to 420 nm and found insignificant change in the PL spectra. Reasonably small excitation wavelength dependency of the emission spectra confirms narrow dispersion in the size of nanobioconjugates. To understand the dynamics of excited electron−hole pair (EHP) recombination, we measured picosecond-resolved PL of the hybrid nanoconjugates. Figure 2b shows picosecond-resolved transient of CHT−CdS (emission wavelength = 550 nm), which is found to be multiexponential in nature with four decay time components (τ_i) with various preexponential values (a_i); 117 ps (66.67%), 784 ps (23.33%) 4.28 ns (6.67%), 46.21 ns (3.33%). The overall PL decay leads to an average decay time $\langle\tau_{av}\rangle = a_1\tau_1 + a_2\tau_2 + a_3\tau_3 = 2.07$ ns. Although, a detail physical or mathematical model of the carrier recombination dynamics of II−VI semiconductor nanocrystals upon photoexcitation is lacking in the present literature,[45,46] a recent attempt from our group has been made[47] to rationalize picosecond dynamics of PL decay of CdS nanoparticles suspended in reverse micellar solution. Relatively faster dynamics (117 ps and 4.28 ns) in the PL-decay have been discussed[47] in the context of controversial "phonon bottleneck" effect.[46] As pointed out in the literature,[45,48] another possibility of the faster PL-decay dynamics is nonradiative recombination to the underlying trap states.

A more precise determination of the average particle size and size distribution was performed via TEM analysis. Figure 3a shows the HRTEM micrograph of the CHT−CdS conjugates at 25 K magnification. The TEM images reveal that the nanobioconjugates are almost spherical in shape. According to a statistical analysis of the TEM results, the CdS NPs have an average particle size of 3.0 nm with a standard deviation of 0.7 nm. The size of conjugates obtained from TEM is slightly smaller than that found by absorption spectrum. The observation of higher diameter of CdS−CHT conjugates as revealed from the absorption and TEM studies compared to the lower estimated value from mass spectrometric analysis suggests that the excess Cd^{+2} ions gets noncovalently attached to the surface of the CdS nanoparticle. The selected area electron diffraction (SAED) pattern simultaneously obtained in the TEM measurement (inset

SCHEME 1 Three-Dimensional Structure of CHT[a]

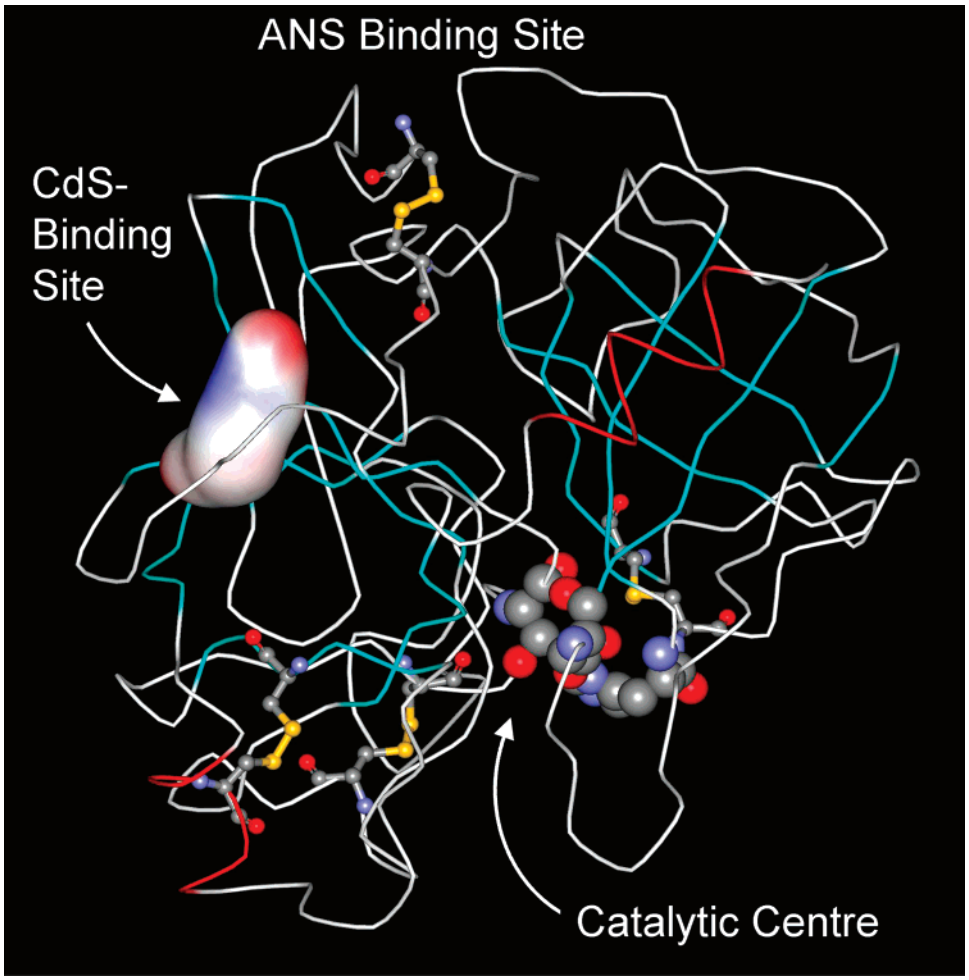

[a] The possible site for CdS attachment indicates the position of the Cys136-Cys201 disulfide bond. Nucleation of the nanocrystal is likely to occur in this site (see text). The solvent accessible surface area (SASA) of the binding site is also shown. Ball and stick models are used to indicate other disulfide bonds of the protein. The coordinates of the CHT structure are downloaded from the Protein Data Bank (ID code 2CHA) and processed with Weblab Viewerlite software.

of Figure 3a) showed three distinct diffraction rings corresponding to the interplanar spacing of 3.12, 1.99, and 1.57 Å, which were assignable to diffractions from (101), (110), and (202) planes of a hexagonal crystal structure of CdS, respectively. However, lattice fringes could not be seen due to blurring of the image when the electron beam was focused on a single nanoparticle. The elemental composition of the CdS−CHT conjugates was examined using an EDAX spectrometer attached to TEM operated at 200kV. A typical EDAX spectrum (Figure 3b) from the conjugates confirmed the presence of C, O, Cd, and S. The Cd:S atomic ratio of 2:1 is consistent with our experimental stoichiometric CdS within experimental error.

In order to investigate the possibility of any structural perturbation of CHT before and after formation of the conjugates, we carried out circular dichroism (CD) studies. Figure 4a shows CD spectra of CHT in phosphate buffer (pH= 7.0) and CdS−CHT in water (pH = 4.5). It is clearly evident from Figure 4a that CD spectrum of CHT remains essentially similar to that of the CdS−CHT conjugates confirming no perturbation in the secondary structure of the protein after the conjugation of CdS nanoparticles. We also investigated the functionality of the enzyme in its native state and conjugated to CdS nanoparticles by measuring their enzymatic activity on a substrate AAF−AMC and recording the rate of formation of AMC−product. We found that the activity of the enzyme in the CdS−CHT conjugates was reduced by 2 times as compared to that in the pure CHT (Figure 4b). This retardation of the enzymatic activity in CdS−CHT conjugates could be attributed to the immobilization of the enzyme upon covalent conjugation to CdS nanoparticles.[49]

The stereoview of CHT is shown in Scheme 1. The enzyme, isolated from bovine pancreas, belongs to a class of digestive serine protease, and has biological function of hydrolyzing polypeptide chains. It is well-known from the crystalline structure of α-chymotrypsin that it has total 5 disulfide bonds (protein data bank, ID code 2CHA). Out of five disulfides, two (Cys1-Cys122 and Cys42-Cys58) are close (within 8 Å) to the enzymatic active site (Scheme 1) and one (Cys191-Cys220) is close to the well-known surface binding site of a fluorescent probe ANS (Scheme 1). The two remaining disulfide bonds (Cys136-Cys201 and Cys168-Cys182) are away from both enzymatic site and ANS binding site. Upon interaction of CdS−CHT conjugates with ANS, we found the emission spectrum to be exactly similar to that of ANS bound to CHT alone indicating that the ANS binding site is not used for hosting CdS nanocrystals. This rules out the possibility of disulfide bonds (Cys1-Cys122 and Cys42-Cys58) for the formation of CdS NPs. Also from the enzymatic activity studies, we found the activity of the enzyme to be only slightly retarded in CdS−CHT conjugates as compared to CHT alone under the structural integrity of CHT. The observation is consistent with the fact that the active site of CHT in the CdS−CHT is completely

available to the substrate of the enzyme and hence rules out the possibility of the disulfide bond (Cys191-Cys220) close to the enzymatic center for the formation of nanobioconjugates. This leaves only two options (Cys136-Cys201 and Cys168-Cys182) for the possible location of CdS nanocrystal formation, which are away from both ANS binding site and enzymatic active site and significantly exposed to the solvent environment (Scheme 1). We calculated the solvent accessible surface area (SASA) of the two sites using the Weblab viewerlite software and found to have values 188.83 and 180.26 $Å^2$ for Cys136-Cys201 (site A) and Cys168-Cys182 (site B), respectively. The higher SASA value of the site A compared to that of the site B makes the former site more favorable for CdS conjugation. It is expected that TCEP, being soluble in water will have much more easy access to that solvent exposed disulfide bond which is having a higher SASA value for reducing the disulfide bond. Thus, we expect that the reduction of the disulfide bond (Cys136-Cys201) takes place readily at this site due to its easy accessibility by TCEP and the subsequent nucleation and growth of CdS NPs occur at this site. The possible site of the CHT for the CdS attachment is shown in Scheme 1.

Conclusion

We report synthesis of water-soluble CdS nanoparticles directly conjugated to a macromolecular protein α-chymotrypsin (CHT). Our synthesis method employs aqueous chemistry at ambient conditions, and we obtain well-dispersed, protein-conjugated CdS nanoparticles of average diameter 3 nm. MALDI mass spectrometry confirmed the strong conjugation of CHT to CdS nanoparticles through covalent bonding in the conjugates and energy dispersive X-ray elemental analysis (EDAX) verified the composition of the CdS−protein conjugates. The structural information of CHT before and after the conjugation of CdS nanoparticles was obtained through circular dichroism (CD) spectroscopy. We found no perturbation in the secondary structure of the protein in CdS−CHT conjugates when compared to that of CHT alone. The functional integrity of CHT conjugated to CdS nanoparticles was confirmed by monitoring the enzymatic activities of CHT alone and CHT-conjugated to CdS nanoparticles by using UV−vis absorption spectroscopy. The unique properties of these nanoparticle-bioconjugates may find their widespread applications in areas ranging from optoelectronics and biosensors to targeted therapeutic agents. The attachment of CdS nanoparticles to an enzyme with its structural and functional integrity may have impact in the future research on nanobio interface.

Acknowledgment. S.S.N. and R.S. thank CSIR and UGC, respectively, for fellowships. We thank DST for financial grant (SR/FTP/PS-05/2004).

References and Notes

(1) Henglein, A. *Chem. Rev.* **1989**, *89*, 1861−1873.
(2) Alivisatos, A. P. *J. Phys Chem.* **1996**, *100*, 13226−13239.
(3) Bawendi, M. G.; Brus, L. E. *Ann. Rev. Phys. Chem.* **1990**, *41*, 477−496.
(4) Steigerwald, M. L.; Brus, L. E. *Acc. Chem. Res.* **1990**, *23*, 183−188.
(5) Wang, Y. *Acc. Chem. Res.* **1991**, *24*, 133−139.
(6) Yanagida, S.; Kawakami, H.; Midori, Y.; Kizumoto, H.; Pac, C.; Wada, Y. *Bull. Chem. Soc. Japan* **1995**, *68*, 1811−1823.
(7) Bruchez, M. J.; Moronne, M.; Gin, P.; Weiss, S.; Alivisatos, A. P. *Science* **1998**, *281*, 2013−2016.
(8) Chan, W. C. W.; Nie, S. *Science* **1998**, *281*, 2016−2018.
(9) Mirkin, C. A.; Letsinger, R. L.; Mucic, R. C.; Storhoff, J. J. *Nature* **1996**, *382*, 607−609.
(10) Alivisatos, A. P.; Johnsson, K. P.; Peng, X.; Wilson, T. E.; Loweth, C. J.; Bruchez, M. P.; Schultz, P. G. *Nature* **1996**, *382*, 609−611.
(11) Mahtab, R.; Rogers, J. P.; Singleton, C. P.; Murphy, C. J. *J. Am. Chem. Soc.* **1996**, *118*, 7028−7032.
(12) Mahtab, R.; Rogers, J. P.; Murphy, C. J. *J. Am. Chem. Soc.* **1995**, *117*, 9099−9100.
(13) Alivisatos, P. *Nat. Biotechnol.* **2004**, *22*, 47−52.
(14) Yoshimura, H. *Colloids Surf. A: Physicochem. Eng. Aspects* **2006**, *282−283*, 464−470.
(15) Murray, C. B.; Norris, D. J.; Bawendi, M. G. *J. Am. Chem. Soc.* **1993**, *115*, 8706−8715.
(16) Katari, J. E. B.; Colvin, V. L.; Alivisatos, A. P. *J. Phys. Chem.* **1994**, *98*, 4109−4117.
(17) Steigerwald, M. L.; Alivisatos, A. P.; Gibson, J. M.; Harris, T. D.; Kortan, R.; Muller, A. J.; Thayer, A. M.; Duncan, T. M.; Douglas, D. C.; Brus, L. E. *J. Am. Chem. Soc.* **1988**, *110*, 3046−3050.
(18) Kortan, A. R.; Hull, R.; Opila, R. L.; Bawendi, M. G.; Steigerwald, M. L.; Carroll, P. J.; Brus, L. E. *J. Am. Chem. Soc.* **1990**, *112*, 1327−1332.
(19) Watzke, H. J.; Fendler, J. H. *J. Phys. Chem.* **1987**, *91*, 854−861.
(20) Niemeyer, C. M. *Angew. Chem., Int. Ed.* **2001**, *40*, 4128−4158.
(21) Niemeyer, C. M. *Angew. Chem., Int. Ed.* **2003**, *42*, 5796−5800.
(22) Niemeyer, C. M.; Burger, W.; Peplies, J. *Angew. Chem., Int. Ed.* **1998**, *37*, 2265−2268.
(23) Connolly, S.; Fitzmaurice, D. *Adv. Mater.* **1999**, *11*, 1202−1205.
(24) Burt, J. L.; Gutiérrez-Wing, C.; Miki-Yoshida, M.; José-Yacamán, M. *Langmuir* **2004**, *20*, 11778−11783.
(25) Wong, K. K. W.; Mann, S. *Adv. Mater.* **1996**, *8*, 928−932.
(26) Yamashita, I.; Hayashi, J.; Hara, M. *Chem. Lett.* **2004**, *33*, 1158−1159.
(27) Yang, L.; Shen, Q.; Zhou, J.; Jiang, K. *Mater. Lett.* **2005**, *59*, 2889−2892.
(28) Meziani, M. J.; Pathak, P.; Harruff, B. A.; Hurezeanu, R.; Sun, Y.-P. *Langmuir* **2005**, *21*, 2008−2011.
(29) Meziani, M. J.; Sun, Y.-P. *J. Am. Chem. Soc.* **2003**, *125*, 8015−8018.
(30) Okuda, M.; Iwahori, K.; Yamashita, I.; Yoshimura, H. *Biotechnol. Bioeng.* **2003**, *84*, 187−194.
(31) Roach, P.; Farrar, D.; Perry, C. C. *J. Am. Chem. Soc.* **2006**, *128*, 3939−3945.
(32) Hong, R.; Fischer, N. O.; Verma, A.; Goodman, C. M.; Emrick, T.; Rotello, V. M. *J. Am. Chem. Soc.* **2004**, *126*, 739−743.
(33) Asuri, P.; Karajanagi, S. S.; Yang, H.; Yim, T.-J.; Kane, R. S.; Dordick, J. S. *Langmuir* **2006**, *22*, 5833−5836.
(34) Vertegel, A. A.; Siegel, R. W.; Dordick, J. S. *Langmuir* **2004**, *20*, 6800−6807.
(35) Lundqvist, M.; Sethson, I.; Jonsson, B.-H. *Langmuir* **2004**, *20*, 10639−10647.
(36) Haugland, R. P. *Handbook of Fluorescent Probes and Research Chemicals*, 7th ed.; Molecular Probes: Eugene, OR, 1996.
(37) Burns, J. A.; Butler, J. C.; Moran, J.; Whitesides, G. M. *J. Org. Chem.* **1991**, *56*, 2648−2650.
(38) Getz, E. B.; Xiao, M.; Chakrabarty, T.; Cooke, R.; Selvin, P. R. *Anal. Biochem.* **1999**, *273*, 73−80.
(39) Kamal, J. K. A.; Xia, T.; Pal, S. K.; Zhao, L.; Zewail, A. H. *Chem. Phys. Lett.* **2004**, *387*, 209−215.
(40) Viswanatha, R.; Sapra, S.; Satpati, B.; Satyam, P. V.; Dev, B. N.; Sarma, D. D. *J. Mater. Chem.* **2004**, *14*, 661−668.
(41) Rossetti, R.; Ellison, J. L.; Gibson, J. M.; Brus, L. E. *J. Chem. Phys.* **1984**, *80*, 4464−4469.
(42) Rossetti, R.; Nakahara, S.; Brus, L. E. *J. Chem. Phys.* **1983**, *79*, 1086−1088.
(43) Moffitt, M.; Eisenberg, A. *Chem. Mater.* **1995**, *7*, 1178−1184.
(44) Brus, L. E. *J. Chem. Phys.* **1984**, *80*, 4403−4409.
(45) Burda, C.; Chen, X.; Narayanan, R.; El-Sayed, M. A. *Chem. Rev.* **2005**, *105*, 1025−1102.
(46) Klimov, V. I. *J. Phys. Chem. B* **2000**, *104*, 6112−6123.
(47) Sarkar, R.; Shaw, A. K.; Narayanan, S. S.; Rothe, C.; Hintschich, S.; Monkman, A.; Pal, S. K. *Opt. Mater.* **2007**, *29*, 1310−1320.
(48) Burda, C.; Link, S.; Mohamed, M.; El-Sayed, M. *J. Phys Chem. B* **2001**, *105*, 12286−12292.
(49) Biswas, R.; Pal, S. K. *Chem. Phys. Lett.* **2004**, *387*, 221−226.